


Perspective

Recent Advances in Mixed-Matrix Membranes for Light Hydrocarbon (C₁–C₃) Separation

Chong Yang Chuah^{1,2,*} and Tae-Hyun Bae^{3,*} 

¹ Department of Chemical Engineering, Universiti Teknologi Petronas, Bandar Seri Iskandar, Perak 32610, Malaysia

² CO₂ Research Centre (CO₂RES), Institute of Contaminant Management, Universiti Teknologi Petronas, Bandar Seri Iskandar, Perak 32610, Malaysia

³ Department of Chemical and Biomolecular Engineering, Korea Advanced Institute of Science and Technology, Daejeon 34141, Korea

* Correspondence: chongyang.chuah@utp.edu.my (C.Y.C.); thbae@kaist.ac.kr (T.-H.B.)

Abstract: Light hydrocarbons, obtained through the petroleum refining process, are used in numerous applications. The separation of the various light hydrocarbons is challenging and expensive due to their similar melting and boiling points. Alternative methods have been investigated to supplement cryogenic distillation, which is energy intensive. Membrane technology, on the other hand, can be an attractive alternative in light hydrocarbon separation as a phase change that is known to be energy-intensive is not required during the separation. In this regard, this study focuses on recent advances in mixed-matrix membranes (MMMs) for light hydrocarbon (C₁–C₃) separation based on gas permeability and selectivity. Moreover, the future research and development direction of MMMs in light hydrocarbon separation is discussed, considering the low intrinsic gas permeability of polymeric membranes.

Keywords: mixed-matrix membrane; zeolite; metal–organic framework; polymers; light hydrocarbon



Citation: Chuah, C.Y.; Bae, T.-H.

Recent Advances in Mixed-Matrix Membranes for Light Hydrocarbon (C₁–C₃) Separation. *Membranes* **2022**, *12*, 201. <https://doi.org/10.3390/membranes12020201>

Academic Editors: Anthony G. Dixon and Yanying Wei

Received: 14 January 2022

Accepted: 6 February 2022

Published: 9 February 2022

Publisher's Note: MDPI stays neutral with regard to jurisdictional claims in published maps and institutional affiliations.



Copyright: © 2022 by the authors. Licensee MDPI, Basel, Switzerland. This article is an open access article distributed under the terms and conditions of the Creative Commons Attribution (CC BY) license (<https://creativecommons.org/licenses/by/4.0/>).

1. Introduction

Light hydrocarbons (specifically methane, acetylene, ethylene, ethane, propylene, and propane) are major raw materials in petrochemical industries. In particular, the increasing demand for polyethylene, poly(vinyl chloride), ethane, and polypropylene, which are used in the production of everyday materials [1], is driving the substantial production of ethylene and propylene (~191 and 120 million tons, respectively, worldwide in 2019) [2–4]. These two hydrocarbons are typically produced through the steam cracking of hydrocarbon sources, such as naphtha, natural gas, coal, and shale gas [5]. Irrespective of the source, the purities of the extracted ethylene and propylene streams should ideally be at least 99.5% [6,7]. The presence of acetylene (>40 ppm) in the ethylene stream, for instance, hampers ethylene polymerization because acetylene could poison the Ziegler–Natta catalyst [8]. This polymerization process is essential because it nullifies contaminants that may trigger side reactions, which could substantially reduce the molecular weight of the resulting polymers [9].

High-pressure cryogenic distillation, a mature technology, has been adopted in industrial operations for light alkene/alkane separation. For example, effective ethylene/ethane separation requires an operating temperature and pressure of –160 °C and 23 bar, respectively, given their similar melting and boiling points (Table 1) [10]; specifically, the boiling and melting points of ethylene and ethane differ by 14 and 15 °C, respectively. Such energy-intensive operating conditions are required for propylene/propane separation as well, because the melting and boiling points of this pair are even more similar (differing by only 6 and 3 °C, respectively). In particular, 75–85% of the input energy is utilized for

the effective production of ethylene and propylene [11]. Thus, alternative technologies for effectively separating light hydrocarbons to isolate specific products are highly desirable.

Various swing adsorption processes have been proposed to alleviate the high energy penalty in conventional (i.e., pressure- or vacuum-based) processes [10–15]. These processes enable hydrocarbon separation at ambient temperature by varying the feed pressure; thus, their energy consumption is relatively low. However, swing adsorption typically entails challenges, such as low recovery, depending on the type of adsorbent used [13,16–21]. In addition, their adsorption–desorption cycling is energy-intensive, which restricts their widespread adoption for light hydrocarbon separation [22]. To overcome these drawbacks, membrane-based gas separation technology (Figure 1) has been developed for cost-effective and energy-efficient light hydrocarbon separation [23]. This approach eliminates the need for phase change as separation is achieved under ambient conditions. Polymeric membranes are the main drivers of this technology as they can be fabricated in large sizes with reasonably high mechanical stability [24,25]. However, because the gas transport mechanism is dominated by the solution-diffusion mechanism, the performance of polymeric membrane-based gas separation is governed by the inevitable trade-off relationship between permeability and selectivity [26,27]. Moreover, molecular sieve membranes, developed using pure zeolites and metal-organic frameworks (MOFs), have low scalability due to their poor mechanical strength [28–30].

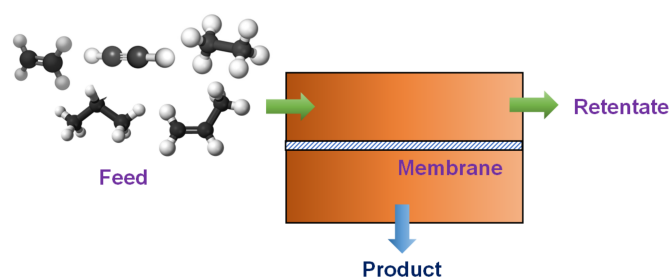


Figure 1. Membranes for gas separation.

Table 1. Properties of light hydrocarbons (C_1 – C_3) [31,32].

Light Hydrocarbon	Normal Boiling Point (°C)	Normal Melting Point (°C)	Critical Pressure (MPa)	Critical Temperature (°C)	Kinetic Diameter (Å) ¹	Van der Waals Diameter (Å) ¹	Polarizability × 10 ²⁵ (cm ³)	Dipole Moment × 10 ¹⁸ (esu cm)	Quadrupole Moment × 10 ²⁶ (esu cm ²)
Methane (CH ₄)	−162	−183	4.6	−83	3.80	3.25	25.9	0	0
Acetylene (C ₂ H ₂)	−84	−81	6.2	−35	3.30	-	33.3	0	-
Ethylene (C ₂ H ₄)	−103	−169	5.1	9	4.16	3.59	42.5	0	1.5
Ethane (C ₂ H ₆)	−89	−184	4.9	32	4.44	3.72	44.3	0	0.7
Propylene (C ₃ H ₆)	−48	−185	4.6	91	4.68 ¹	4.03	62.6	0.4	-
Propane (C ₃ H ₈)	−42	−188	4.3	97	4.30 ¹	4.16	62.9	0.1	-

¹ Hybrid molecular dimension scales based on kinetic diameter and van der Waals diameter are required to obtain a clearer understanding of membrane performance.

Mixed-matrix membranes (MMMs), which combine the advantages of polymeric and molecular sieves (adsorbents), have been a focus of research attention. Numerous papers have reviewed the research on membranes for hydrocarbon separation [2,5,33–35]; therefore, the present study focuses mainly on the performance of MMMs and composite membranes in separating C_1 to C_3 hydrocarbons. In general, the utilization of MOFs as potential fillers for light hydrocarbon separation has been the main focus due to their

higher flexibility in both pore size control and post-synthetic functionalization compared to conventional porous materials, such as zeolites [23]. In addition, their performance with respect to the upper bound limit (C_2H_4/C_2H_6 and C_3H_6/C_3H_8) [36,37] is discussed. Finally, insights on the future research and development direction of MMMs in light hydrocarbon separation are shared.

2. C_2 Hydrocarbon Separation

Membranes in C_2 hydrocarbon separation have been mainly investigated with respect to their potential in C_2H_4/C_2H_6 separation (Table 2). However, although polymeric membranes, especially those commercially available, are robust and processable, they do not exhibit high permeabilities in ethylene/ethane separation. For example, Naghsh et al. [38], Davoodi et al. [39], and Jeroen et al. [40] demonstrated that the C_2H_4 permeabilities of Matrimid[®], cellulose acetate (CA), and polyimide (P84) under ambient conditions were merely 0.26, 0.051, and 0.049 barrer, respectively, which is attributable to their low fractional free volume (FFV). C_2H_4/C_2H_6 selectivities, on the other hand, were reported to be moderate, with values of 3.25, 2.27, and 4.00, respectively. It is expected that the reported selectivity is comparatively higher than those of polymers with large FFV, such as 6FDA-based polymers and PIM-1, as observed in CO_2 separation [24,28,41]. Therefore, these low intrinsic gas permeabilities make the lab-scale (gas chromatography) investigation of such membranes challenging, as it requires specific devices (high-accuracy pressure transducers or thermal conductivity detectors) or conditions (high feed pressure). The advantages of incorporating filler materials into polymeric membranes have been investigated. For instance, Naghsh et al. [38] and Davoodi et al. [39] incorporated amorphous silica nanoparticles into Matrimid[®] and CA membranes, respectively, and investigated their performance in C_2H_4/C_2H_6 separation; the incorporation of 20 wt% silica in these two polymeric membranes was found to increase C_2H_4 permeability by 58% and 76%, with no substantial change in C_2H_6 permeability, in comparison with pure polymer matrix. Although silica nanoparticles are not porous, the residual hydroxyl (–OH) functionalities make interactions with polar C_2H_4 molecules feasible. Furthermore, the incorporation of silica nanoparticles disrupts polymer packing, which increases the FFV and facilitates rapid gas transport.

These advantages notwithstanding, the use of non-porous silica nanoparticles constrains improvements in C_2H_4/C_2H_6 separation performance due to their lack of intrinsic porosity, highlighting the need for the incorporation of porous materials into separation membranes. In this regard, MOFs with coordinative unsaturated open metal sites are of particular interest. These metal sites interact favorably with the π -bond in C_2H_4 , thus facilitating C_2H_4 adsorption. Bachman et al. [42] identified M_2dobdc ($M = Co, Fe, Mg, Mn, Ni, Zn$), which possess reasonable C_2H_4/C_2H_6 selectivity (c.a. 8–12 at 50/50 vol/vol C_2H_4/C_2H_6 and 35 °C, based on ideal adsorbed solution theory [IAST] calculations), as a feasible adsorbent. Studies on MMMs incorporated with M_2dobdc nanocrystals have revealed that the addition of Mg_2dobdc and Mn_2dobdc , unlike Ni_2dobdc and Co_2dobdc , creates undesirable interfacial gaps in the polymer matrix, leading to non-selective gas transport [42,43]. Nevertheless, given their high C_2H_4 adsorption, these M_2dobdc -incorporated MMMs have exhibited large increases in C_2H_4 permeability, making it increasingly likely to surpass the upper bound limit for C_2H_4/C_2H_6 separation. The advantages of incorporating MOFs with open metal sites were also demonstrated by Chuah et al. [44], who used HKUST-1 as the adsorbent; specifically, the incorporation of 20 wt% HKUST-1 in 6FDA-TMPDA membranes substantially improved their C_2H_4 permeability, pushing their performance close to the C_2H_4/C_2H_6 upper bound limit (Figure 2).

MMMs have also been applied in acetylene separation. However, adsorbents with high acetylene/ethylene selectivity are rare [6]. MOFs are generally more favorable for acetylene/ethylene separation than conventional adsorbents, such as zeolites and activated carbon, because MOFs offer more systematic control over pore size (through the selection of ligands with varying strut lengths) and are compatible with pre- and post-synthetic

functionalization. Qian et al. [45] recently demonstrated the C_2H_2/C_2H_4 selectivity of two types of MOF, namely SIFSIX-2-Cu-i and ZRFSIX-2-Ni-i (Figure 3a); this favorable performance is attributable to the presence of MF_6^{2-} moieties ($M = Cu, Ni$), which enables strong interactions with C_2H_2 . Furthermore, poly(ionic liquids) have also been used in this manner given their reasonable C_2H_2 permeability and filler–polymer compatibility [46–48]. Specifically, single-gas permeation experiments have shown that 30 wt% SIFSIX-2-Cu-i and ZRFSIX-2-Ni-i in poly(ionic liquids) improve C_2H_2 permeability by 129% and 100%, respectively (Figure 3b), without a substantial change in C_2H_2/C_2H_4 selectivity.

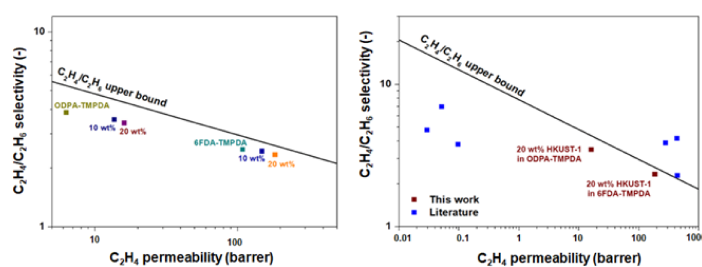


Figure 2. Performance of mixed-matrix membranes (MMMs) with 10 and 20 wt% HKUST-1 loading in ODDA-TMPDA and 6FDA-TMPDA membranes; 20 wt% HKUST-1, whose performance is comparable with those of other membranes reported in previous research, has the potential to surpass the upper bound limit of C_2H_4/C_2H_6 separation. Reprinted with permission from [44], Creative Commons Attribution 4.0.

The feasibility of using MMMs for C_2H_6/CH_4 separation has also been explored in research. In contrast to MOFs, which are effective at C_2H_4/C_2H_6 separation, the applicability of zeolite adsorbents in this separation is relatively less common than in CO_2 separation (e.g., post-combustion or pre-combustion carbon capture) [49,50] due to the comparable polarizability and quadrupole moment of C_2H_4 and C_2H_6 molecules (Table 1). Hence, C_2H_6/CH_4 separation was investigated instead due to a more substantial difference in their polarizabilities. Tirouni et al. [51] investigated C_2H_6/CH_4 separation using polyurethane MMMs incorporated with zeolite 4A and ZSM-5. With this zeolite-based approach, the polarizability of C_2H_6 is higher than that of CH_4 ; accordingly, the permeability of C_2H_6 is also higher than that of CH_4 . However, this approach is not promising due to its low C_2H_6/CH_4 selectivity, which in turn is attributable to the poor compatibility between the polymer matrix and the zeolite particles; specifically, the zeolite–polymer configuration has been reported to exhibit the sieve-in-a-cage morphology [52–55]. These shortcomings can be potentially overcome via post-synthetic treatments, such as the incorporation of silane coupling agents and post-synthetic amine grafting. However, these treatments may jeopardize the effective transport of the desired gas through the membranes [23].

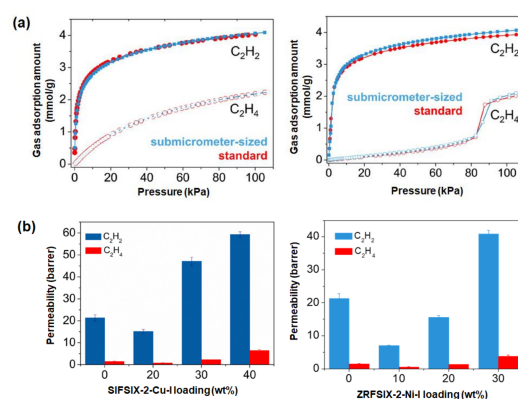


Figure 3. (a) C_2H_2 and C_2H_4 adsorption of SIFSIX-2-Cu-i and ZRFSIX-2-Ni-i at 25 °C; (b) C_2H_2 and

C₂H₄ permeability of MMMs with SIFSIX-2-Cu-i and ZRFSIX-2-Ni-i loading in poly(ionic liquids). Reprinted with permission from [45], copyright 2020, Elsevier.

Table 2. Performance of mixed-matrix membranes (MMMs) in C₂ hydrocarbon separation.

Membrane		Measurement Condition			Gas Permeability (Barrer)				Gas Selectivity		Ref.
Polymer/Support	Filler	Loading (wt%)	Pres. (bar)	Temp. (°C)	C ₂ H ₂	C ₂ H ₄	C ₂ H ₆	CH ₄	C ₂ H ₂ /C ₂ H ₄	C ₂ H ₄ /C ₂ H ₆	
6FDA-DAM	Ni-gallate	20	-	-	-	91	25	-	-	4.13	[56]
6FDA-TMPDA	Co2(dobdc)	33	2	35	-	276	71	-	-	3.89	[42]
6FDA-TMPDA	Ni2(dobdc)	25	0.75	35	-	426	101	-	-	4.22	[42]
6FDA-TMPDA	Mg2(dobdc)	23	2	35	-	1140	431	-	-	2.65	[42]
6FDA-TMPDA	Mn2(dobdc)	13	2	35	-	433	188	-	-	2.30	[42]
6FDA-TMPDA	HKUST-1	20	1	35	-	183	76	-	-	2.41	[44]
α-alumina	Zeolite MFI	-	9	25	-	-	37 ^[1]	6 ^[1]	-	-	[57]
Cellulose Acetate	Silica	30	-	-	-	0.11	0.026	-	-	4.23	[38]
DBzPBI-BuI	ZIF-8	30	2.7	35	-	112	41	-	-	2.73	[58]
Matrimid	Silica	20	3	30	-	0.42	0.07	-	-	6	[39]
Nylon	Boron Nitride ^[2]	-	2	-	-	160 ^[1]	1.9 ^[1]	-	-	84.2	[29]
ODPA-TMPDA	HKUST-1	20	1	35	-	16	4.7	-	-	3.40	[44]
P1-1 ^[3]	SIFSIX-2-Cu-i	30	1.5	-	45	2.1	-	-	21.4	-	[45]
P1-1 ^[3]	ZRFSIX-2-Ni-i	30	1.5	-	15	1.3	-	-	11.5	-	[45]
P84	HKUST-1	20	5	-	-	0.052	0.0075	-	-	6.93	[59]
P84	Fe-BTC	20	5	-	-	0.03	0.0052	-	-	5.77	[40]
P84	MIL-53	20	5	-	-	0.096	0.027	-	-	3.56	[40]
Polystyrene	Fullerene	1	-	35	-	0.58	0.34	-	-	1.71	[60]
Polyurethane	Zeolite 4A	10	2	30	-	-	66.6	53	-	-	[51]
Polyurethane	ZSM-5	20	2	30	-	-	71.3	32.3	-	-	[51]
PPEES	ZIF-8	30	1	-	-	3.2	1.0	-	-	3.2	[61]
PVDF	Ag-Al/NMA	-	0.1	25	-	450	30	-	-	15	[62]

^[1] Permeance in GPU; ^[2] incorporated with reactive ionic liquid (RIL); ^[3] P1-1: (ATMA)(BF₄)/PEG₅₀₀ = 1:1 (2-(acryloyloxy)ethyl-trimethylammonium tetrafluoroborate)/poly(ethylene glycol) methyl ether methacrylate; 6FDA = 4,4'-(hexafluoroisopropylidene)diphthalic anhydride; DAM = 2,4-diaminomesitylene; DBzPBI-BuI = substituted polybenzimidazole; ODPDA = 4,4'-oxydiphthalic anhydride; PPEES = poly(1,4-phenylene ether-ether-sulfone); PVDF = polyvinylidene fluoride; TMPDA = 2,4,6-trimethyl-*m*-phenylenediamine.

3. C₃ Hydrocarbon Separation

C₃ hydrocarbon separation has primarily been examined for the propylene/propane (C₃H₆/C₃H₈) gas pair (Table 3), with few studies examining the C₃H₈/CH₄ gas pair. As discussed in Section 2, commercial polymer membranes do not exhibit intrinsically high C₃H₆ permeability and C₃H₆/C₃H₈ selectivity due to their considerably larger kinetic diameter compared with other common gaseous molecules, such as CO₂, N₂, C₂H₄, and C₂H₆. Naghsh et al. [38] and Davoodi et al. [39] demonstrated that the C₂H₆ permeabilities of Matrimid[®] and CA under ambient conditions were as low as 0.09 and 0.046 barrer, respectively, due to their low FFV. Thus, it is highly desirable to use polyimide membranes with high intrinsic C₃H₆ permeabilities, such as 6FDA-based polymers and rubbery polymers (e.g., polydimethylsiloxane (PDMS)) and cross-linked poly(ethylene oxide) (XLPEO)) to achieve sufficient flux for gas separation.

Regarding other porous materials, the effectiveness of ZIF-8 (ZIF = zeolitic imidazolate framework), which is generally stable toward water and organic solvents (e.g., methanol), in C_3H_6/C_3H_8 separation has been investigated. Based on single-crystal X-ray diffraction data, the aperture of ZIF-8 has been reported to be 3.4 \AA [63], which is fairly flexible compared with rigid frameworks (e.g., zeolites and zeotype materials). Thus, considering the flexibility of the ligands present in ZIF-8, Zhang et al. [64] estimated (revised) the effective aperture size. According to the adsorption kinetics of C_3H_6 and C_3H_8 , C_3H_6 has a shorter equilibration time than C_3H_8 (Figure 4a), indicating a potential means of size discrimination between C_3H_6 and C_3H_8 . However, a precise cut-off for the ZIF-8 aperture size cannot be determined. As an alternative, based on the diffusivities of gaseous molecules against pure ZIF-8 membrane (as calculated from the Maxwell model [23,65]), the diffusion selectivity of C_3H_6/C_3H_8 has been reported to exceed 100 at $35 \text{ }^\circ\text{C}$ (Figure 4b); this result indicates the feasibility of using the ZIF-8 aperture size to achieve effective molecular sieving between C_3H_6 and C_3H_8 . As evident from Table 1, kinetic diameter alone is not satisfactory for characterizing the molecular diffusion for selective C_3H_6 transport. Thus, as suggested by Zhang et al. [64], a hybrid molecular dimension scale (i.e., a combination of kinetic and van der Waals diameters) is required to effectively explain the feasibility of ZIF-8 to perform effective C_3H_6/C_3H_8 separation.

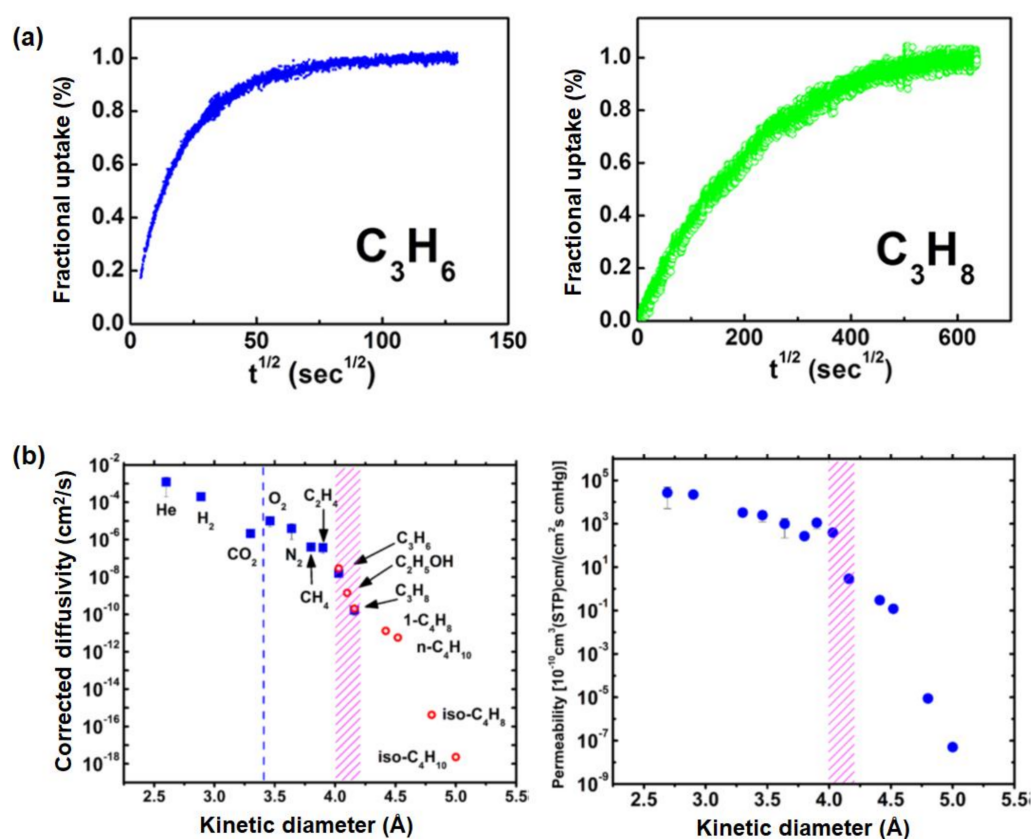


Figure 4. (a) Adsorption kinetics of C_3H_6 and C_3H_8 with ZIF-8 at $35 \text{ }^\circ\text{C}$; (b) corrected diffusivities and permeability of pure ZIF-8 membrane at $35 \text{ }^\circ\text{C}$. Reprinted with permission from [64], copyright 2012, American Chemical Society.

Numerous researchers have investigated the use of ZIF-8 for effective C_3H_6/C_3H_8 separation. The first widely known investigation of ZIF-8 as a filler in MMMs for C_3H_6/C_3H_8 separation was conducted by Zhang et al. [66]. Based on the gas adsorption isotherms and adsorption kinetics of both C_3H_6 and C_3H_8 , their sorption capacities and fractional uptake are comparable. The incorporation of 48 wt% ZIF-8 in 6FDA-TMPDA membranes was found to increase the C_3H_6 permeability and C_3H_6/C_3H_8 selectivity by 258% and 150%,

respectively. These conflicting results are attributable to the difficulty of accurately characterizing the adsorption kinetics (i.e., determining the mass and heat transfer resistance and particle size) during the equilibrium gas adsorption measurements [12,67].

Efforts have also been made to improve the separation performance of ZIF-8-containing MMMs. Specifically, polymers other than 6FDA-TMPDA [68] have been investigated with the aim of surpassing the upper bound limit for C_3H_6/C_3H_8 separation. For example, Ma et al. [69] examined the use of PIM-6FDA-OH, which possesses higher C_3H_6/C_3H_8 selectivity (30 vs 12 for 6FDA-TMPDA) due to the hydroxyl (–OH) group. As evidenced by X-ray photon spectroscopy (XPS) data (Figure 5a), hydrogen bonding (N . . . H–O) between the nitrogen moiety in the ZIF-8 ligand and the –OH group in the polymer improves the compatibility between the filler and the polymer (Figure 5b), in turn improving the C_3H_6 permeability and C_3H_6/C_3H_8 selectivity by 1.086% and 43%, respectively (Figure 5c), at 65 wt% ZIF-8. The incorporation of ZIF-8 in rubbery polymers, such as PDMS and XLPEO, has also been explored given their high C_3H_6 permeability [70,71], but these compounds have yet to be used in industrial operations due to their low inherent brittleness [24].

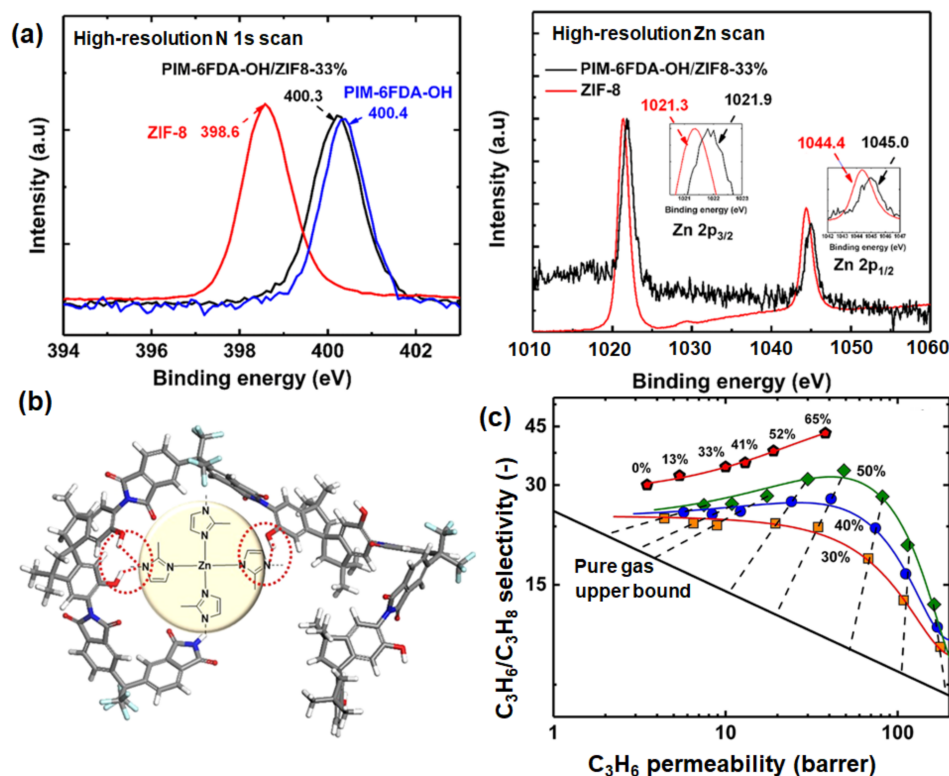


Figure 5. (a) Effect of incorporating ZIF-8 in PIM-6FDA-OH on the Zn and N signals in XPS spectra. (b) Illustration of the proposed mechanism, based on hydrogen bonding between ZIF-8 and the polymer (PIM-6FDA-OH); (c) C_3H_6/C_3H_8 separation performance with varying ZIF-8 loading. Theoretical prediction at 30 wt% (orange), 40 wt% (blue), and 50 wt% (green) ZIF-8 are illustrated for comparison. Reprinted with permission from [69], copyright 2018, American Chemical Society.

Other porous materials have also been explored for C_3H_6/C_3H_8 separation. For instance, cobalt-substituted ZIF-8 (ZIF-67) has been proposed to be more efficient in this regard than ZIF-8 because the Co–N bond in ZIF-67 is stiffer than the Zn–N bond in ZIF-8. In particular, due to the higher electronegativity of Co compared with Zn, the generation of a stiffer ionic bond has the potential to restrict the flipping motion of the organic ligands present in the respective MOFs (Figure 6a) [72–74]. An et al. [75] demonstrated that the incorporation of 20 wt% ZIF-67 in 6FDA-TMPDA improved the C_3H_6/C_3H_8 selectivity by 165%, whereas a comparable ZIF-8 incorporation resulted in an 83% improvement. Furthermore, Oh et al. [76] developed Co²⁺ and Zn²⁺ mixed-metal hybrids (ZIF-8-67) to

take advantage of the benefits of both fillers. A comparison study of ZIF-8, ZIF-67, and ZIF-8-67 revealed that ZIF-8-67 could improve C_3H_6 permeability to a much larger extent than could the ZIF-8 and ZIF-67 frameworks (Figure 6b). The use of composite fillers, such as ZIF-67 with porous graphene oxide (GO) [77], has also been explored. The creation of three-dimensional architectures with MOFs and GO has been reported to increase the accessible surface area due to the favorable interactions between the functional groups in GO and the ligands in MOFs [78–80].

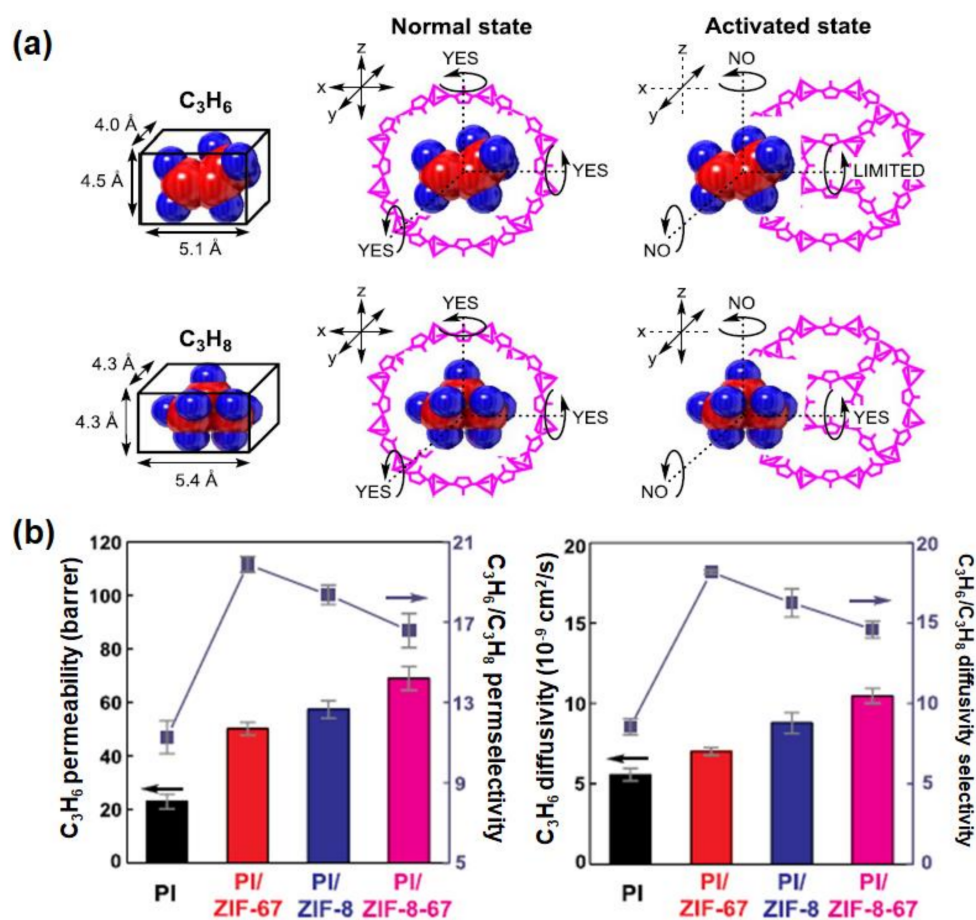


Figure 6. (a) Illustration of the effect of transport of C_3H_6 and C_3H_8 upon passing through the pores of ZIF-67. Reprinted with permission from [75], copyright 2017, Elsevier; (b) effect of incorporating ZIF-67, ZIF-8, and ZIF-8-67 at 21.9 wt% loading in polyimide (PI) on C_3H_6 permeability, C_3H_6/C_3H_8 permeability selectivity, C_3H_6 diffusivity, and C_3H_6/C_3H_8 diffusivity selectivity. Reprinted with permission from [76], copyright 2020 Elsevier.

Frameworks other than those involving ZIFs have also been investigated in previous research. For example, Liu et al. [81] examined the potential of Zr-*fum*-*fcu*-MOF crystals in C_3H_6/C_3H_8 separation and found that the resulting C_3H_6/C_3H_8 sorption selectivity is comparable with that of ZIF-8, and a pore aperture size of 3.3–4.6 Å was found to further improve the C_3H_6/C_3H_8 diffusion selectivity. Furthermore, it has been postulated that C_3H_8 has a comparatively higher energy barrier to pass through Zr-*fum*-*fcu*-MOF crystals than does C_3H_6 , due to the C–C bond rotation of C_3H_8 . Similarly, Lee et al. [82] developed defect-engineered MOFs derived from hydrolytically-stable [83] UiO-66 to create additional sorption sites for effective C_3H_6/C_3H_8 separation; their defect-engineered UiO-66-based MMM significantly improved C_3H_6 permeance (1.005%) relative to the control (UiO-66-based MMM, 308%), without substantially jeopardizing the C_3H_6/C_3H_8 selectivity.

Table 3. Performance of mixed-matrix membranes (MMMs) in C₃ hydrocarbon separation.

Membrane			Measurement Condition		Gas Permeability (barrer)			Gas Selectivity	Ref.
Polymer/ Support	Filler	Loading (wt%)	Pres. (bar)	Temp. (°C)	C ₃ H ₆	C ₃ H ₈	CH ₄	C ₃ H ₆ /C ₃ H ₈	
6FDA-Durene	ZIF-8	30	2	35	49	2.8	-	17.5	[71]
6FDA-TMPDA	UiO-66	20	2	35	87.4	8.9	-	9.82	[82]
6FDA-TMPDA	UIO-TF36	20	2	35	236.5	24.5	-	9.65	[82]
6FDA-TMPDA	ZIF-67	20	2	35	47.8	3.7	-	14.06	[77]
6FDA-TMPDA	ZIF-67	20	-	35	34.1	1.1	-	31.00	[75]
6FDA-TMPPDA	ZIF-67/GO (ZGO67)	20	2	35	43.1	3.1	-	13.90	[77]
6FDA-TMPDA	ZIF-8	20	-	35	27.7	1.8	-	15.39	[75]
6FDA-TMPDA	ZIF-8	48	2	35	52	2.4	-	21.67	[69]
6FDA-TMPDA	ZIF-8	48	2	35	56.2	1.8	-	31.22	[66]
6FDA-TMPDA	ZIF-8	30	2	35	15	1	21	15.00	[68]
6FDA-TMPDA	ZIF-8	30	2	35	10 ^[1]	1.5 ^[1]	-	6.67	[68]
6FDA-TMPDA	ZIF-8	30	2	35	35	1.7	-	20.59	[71]
6FDA-TMPDA	ZIF-8-67	21.9	2	35	65	3.9	-	16.67	[76]
6FDA-TMPDA	ZPGO67	20	2	35	55.4	3.9	-	14.21	[77]
6FDA-TMPDA	Zr-fum-fcu-MOF	15	1	35	40.4	2.8	-	14.43	[81]
6FDA-TMPDA (with PDMS)	ZIF-8	30	2	35	6 ^[1]	0.4 ^[1]	-	15.00	[68]
α-alumina	Zeolite MFI	-	9	25	-	300	6 ^[2]	-	[57]
Cellulose Acetate	silica	30	-	-	0.092	0.018	-	5.11	[38]
Comb copolymers	AgBF ₄ /MgO nanosheet (3:7)	-	-	-	11.8 ^[1]	0.9 ^[1]	-	13.11	[84]
DBzPBI-BuI	ZIF-8	30	2.7	35	11	0.4	-	27.50	[58]
Ethyl Cellulose	Fullerene	10	1	-	10	3	-	3.33	[85]
Matrimid	Silica	20	3	30	0.16	0.008	-	20.00	[39]
PEBAX® 1657	ZIF-8	30	2	35	195	78	-	2.50	[71]
PEBAX® 2533	ZIF-8	20	2	35	420	220	-	1.91	[71]

Table 3. Cont.

Membrane			Measurement Condition		Gas Permeability (barrer)			Gas Selectivity	Ref.
Polymer/Support	Filler	Loading (wt%)	Pres. (bar)	Temp. (°C)	C ₃ H ₆	C ₃ H ₈	CH ₄	C ₃ H ₆ /C ₃ H ₈	
PDMS	ACN-N	10	4	35	-	11,000	1000	-	[86]
PDMS	ACN-O	10	4	35	-	13,000	1050	-	[86]
PDMS	SiO ₂	10	5	35	9800	-	-	-	[87]
PDMS	ZIF-8	20	2	-	-	160 ^[1]	-	-	[70]
PIM-6FDA-OH	ZIF-8	65	2	35	35	1.1	-	31.81	[69]
Polyurethane	Zeolite 4A	10	2	30	-	78	53	-	[51]
Polyurethane	ZSM-5	20	2	30	-	71.3	32.3	-	[51]
PVAc	ZIF-8	40	2	35	24	2	-	12	[71]
XLPEO	ZIF-8	42	2	35	28	1.9	-	14.73	[71]
XLPEO	ZIF-8-IT	20	-	35	11.6	1.8	-	6.44	[88]
XLPEO	ZIF-8-NC	20	-	35	13.8	1.9	-	7.26	[88]
XLPEO	ZIF-8-NR	20	-	35	16.6	1.8	-	9.22	[88]
XLPEO	ZIF-8-OP	20	-	35	12.5	2.2	-	5.68	[88]
XLPEO	ZIF-8-RD	20	-	35	10.2	1.9	-	5.37	[88]

^[1] Permeance in GPU; 6FDA = 4,4'-(hexafluoroisopropylidene)diphthalic anhydride; CAN = adsorptive carbon nanoparticles; DBzPBI-BuI = substituted polybenzimidazole; IT = interpenetration twin; NC = nanocube; NR = nanorod; OP = octagonal plate; PIM = polymer of intrinsic microporosity; PDMS = polydimethylsiloxane; PVAc = polyvinyl acetate; TF = trifluoroacetic acid; TMPDA = 2,4,6-trimethyl-m-phenylenediamine; XLPEO = crosslinked poly(ethylene oxide).

4. Comparison of Membrane Performance against the Upper Bound

In this study, the hydrocarbon separation performance of membranes is benchmarked against the upper bound curve for C₂H₄/C₂H₆ and C₃H₆/C₃H₈ separation, based on the data in Tables 2 and 3, respectively. The parameters used to obtain the upper bound plot (Figure 7) are listed in Table 4. The results reveal that achieving excellent light hydrocarbon separation performance is highly challenging. For example, the trend in Figure 7a indicates that the upper bound limit could easily be surpassed by using polymeric membranes with M₂dobdc series fillers, considering their high C₂H₄ adsorption and C₂H₄/C₂H₆ selectivity (based on IAST calculations). However, MOFs with open metal sites generally exhibit poor hydrolytic stability, which may affect their long-term separation performance. The incorporation of deep eutectic solvents (DES) into polymeric membrane [62] has been proven to be feasible in substantially improving C₂H₄/C₂H₆ selectivity, the challenges of developing cost-effective and highly stable DES notwithstanding [89,90]. As discussed in Section 3, the use of ZIF-8 as porous material in membranes for C₃H₆/C₃H₈ separation has been proven effective, as ZIF-8 substantially improves C₃H₆/C₃H₈ selectivity. Thus, the incorporation of ZIF-8 in polymeric membranes has the potential to surpass the C₃H₆/C₃H₈ upper bound limit, as indicated in Figure 7b.

Table 4. Parameters used to obtain the upper bound for C₂H₄/C₂H₆ and C₃H₆/C₃H₈ separation.

Upper Bound Curve	2003 (2013) ^[1]	
	λ ^[2]	β ^[2]
C ₂ H ₄ /C ₂ H ₆	0.14	7.3
C ₃ H ₆ /C ₃ H ₈	0.17	20.4

^[1] The upper bounds for C₂H₄/C₂H₆ and C₃H₆/C₃H₈ are based on the data obtained in 2013 and 2003, respectively; ^[2] λ and β are described as the slope and front factor of the upper bound line, for which the relation between permeability and selectivity can be correlated as follows: $\alpha = (\beta/P^\lambda)$.

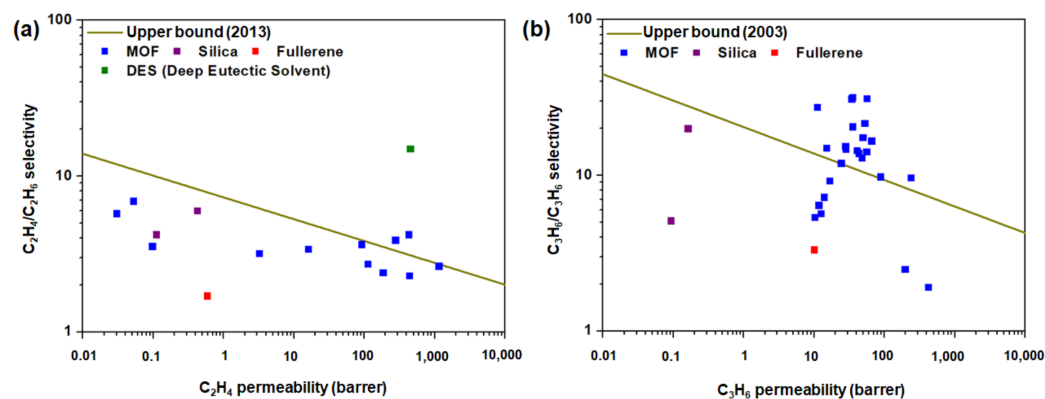


Figure 7. Performance of MMMs in (a) C_2H_4/C_2H_6 and (b) C_3H_6/C_3H_8 separation. The data points indicated in Panels (a) and (b) are from Tables 2 and 3, respectively. The parameters used to generate the upper bound line [36,37] are summarized in Table 4.

5. Conclusions and Future Perspectives

This perspective paper presents an overview of MMMs used for C_2H_4/C_2H_6 and C_3H_6/C_3H_8 separation. Such light hydrocarbon separations are generally challenging due to the similar polarizabilities, kinetic diameters, and van der Waals diameters of the adsorbates, which make it difficult to realize high selectivity. Moreover, because light hydrocarbon molecules are bulkier than carbon dioxide, nitrogen, and methane (which have been extensively investigated for CO_2 separation [23,28,91]), membranes with high FFV are highly desirable for separation. Thus, most relevant studies have investigated high-performance polyimides, namely 6FDA-based polymers and PIMs [44,92,93]. However, these polymers require extensive monomer purification, making their large-scale fabrication difficult [53]. Composite membranes are thus a feasible alternative for light hydrocarbon separation. This can be potentially achieved with the utilization of porous fillers possessing large accessible surface areas that are not limited to zeolites and MOFs, as they can effectively increase the diffusion rates of gas-molecule MMMs.

Future efforts should focus on the investigation of MMMs for acetylene separation. Acetylene is typically produced via the thermal cracking of CH_4 and typically contains CO_2 as the byproduct. Acetylene is also present as an impurity in C_2H_4 production, which tends to disrupt the effective polymerization of C_2H_4 . Acetylene separation is largely reliant on the use of adsorbents, but effective membrane-based separation is difficult because of the comparable properties of the adsorbates (Table 1). Nevertheless, the membrane performance of MMMs can be expected to improve through the use of porous materials proven to be effective in previous studies.

Author Contributions: Writing—draft preparation, review and editing, C.Y.C. and T.-H.B. All authors have read and agreed to the published version of the manuscript.

Funding: This work is supported by the Universiti Teknologi Petronas (UTP) and National Research Foundation of Korea (NRF), grant funded by the Korean government MSIT (Reference number: 2021M313A1084977).

Institutional Review Board Statement: Not applicable.

Informed Consent Statement: Not applicable.

Data Availability Statement: Not applicable.

Conflicts of Interest: The authors declare no conflict of interest.

References

1. Sholl, D.S.; Lively, R.P. Seven chemical separations to change the world. *Nature* **2016**, *532*, 435. [CrossRef]
2. Ren, Y.; Liang, X.; Dou, H.; Ye, C.; Guo, Z.; Wang, J.; Pan, Y.; Wu, H.; Guiver, M.D.; Jiang, Z. Membrane-Based Olefin/Paraffin Separations. *Adv. Sci.* **2020**, *7*, 2001398. [CrossRef] [PubMed]
3. Garside, M. Global Production Capacity of Propylene 2018–2030. Available online: <https://www.statista.com/statistics/1065879/global-propylene-production-capacity/> (accessed on 3 July 2021).
4. Garside, M. Global Production Capacity of Ethylene 2014–2024. Available online: <https://www.statista.com/statistics/1067372/global-ethylene-production-capacity/#:~:text=The%20production%20capacity%20of%20ubiquitous,to%20283%20million%20metric%20tons> (accessed on 3 July 2021).
5. Chen, X.Y.; Xiao, A.; Rodrigue, D. Polymer-based Membranes for Propylene/Propane Separation. *Sep. Purif. Rev.* **2021**, *51*, 1–13. [CrossRef]
6. Lee, J.; Chuah, C.Y.; Kim, J.; Kim, Y.; Ko, N.; Seo, Y.; Kim, K.; Bae, T.H.; Lee, E. Separation of acetylene from carbon dioxide and ethylene by a water-stable microporous metal–organic framework with aligned imidazolium groups inside the channels. *Angew. Chem. Int. Ed.* **2018**, *130*, 7995–7999. [CrossRef]
7. Nitzsche, R.; Budzinski, M.; Gröngroft, A. Techno-economic assessment of a wood-based biorefinery concept for the production of polymer-grade ethylene, organosolv lignin and fuel. *Bioresour. Technol.* **2016**, *200*, 928–939. [CrossRef]
8. Wen, H.-M.; Li, B.; Wang, H.; Krishna, R.; Chen, B. High acetylene/ethylene separation in a microporous zinc (II) metal–organic framework with low binding energy. *Chem. Commun.* **2016**, *52*, 1166–1169. [CrossRef]
9. Drobny, J.G. 4-Fluoroelastomer Monomers. In *Fluoroelastomers Handbook*, 2nd ed.; Drobny, J.G., Ed.; William Andrew Publishing: Norwich, NY, USA, 2016; pp. 29–40. [CrossRef]
10. Van Miltenburg, A.; Zhu, W.; Kapteijn, F.; Moulijn, J. Adsorptive separation of light olefin/paraffin mixtures. *Chem. Eng. Res. Des.* **2006**, *84*, 350–354. [CrossRef]
11. Liang, W.; Zhang, Y.; Wang, X.; Wu, Y.; Zhou, X.; Xiao, J.; Li, Y.; Wang, H.; Li, Z. Asphalt-derived high surface area activated porous carbons for the effective adsorption separation of ethane and ethylene. *Chem. Eng. Sci.* **2017**, *162*, 192–202. [CrossRef]
12. Chuah, C.Y.; Lee, Y.; Bae, T.-H. Potential of adsorbents and membranes for SF₆ capture and recovery: A review. *Chem. Eng. J.* **2020**, *404*, 126577. [CrossRef]
13. Alcántara-Avila, J.R.; Gómez-Castro, F.I.; Segovia-Hernández, J.G.; Sotowa, K.-I.; Horikawa, T. Optimal design of cryogenic distillation columns with side heat pumps for the propylene/propane separation. *Chem. Eng. Process. Process Intensif.* **2014**, *82*, 112–122. [CrossRef]
14. Yang, Y.; Chuah, C.Y.; Bae, T.-H. Polyamine-appended porous organic polymers for efficient post-combustion CO₂ capture. *Chem. Eng. J.* **2019**, *358*, 1227–1234. [CrossRef]
15. Yang, Y.; Chuah, C.Y.; Bae, T.-H. Highly efficient carbon dioxide capture in diethylenetriamine-appended porous organic polymers: Investigation of structural variations of chloromethyl monomers. *J. Ind. Eng. Chem.* **2020**, *88*, 207–214. [CrossRef]
16. Lin, R.-B.; Li, L.; Zhou, H.-L.; Wu, H.; He, C.; Li, S.; Krishna, R.; Li, J.; Zhou, W.; Chen, B. Molecular sieving of ethylene from ethane using a rigid metal–organic framework. *Nat. Mater.* **2018**, *17*, 1128–1133. [CrossRef]
17. Aguado, S.; Bergeret, G.R.; Daniel, C.; Farrusseng, D. Absolute molecular sieve separation of ethylene/ethane mixtures with silver zeolite A. *J. Am. Chem. Soc.* **2012**, *134*, 14635–14637. [CrossRef]
18. Anson, A.; Wang, Y.; Lin, C.; Kuznicki, T.; Kuznicki, S. Adsorption of ethane and ethylene on modified ETS-10. *Chem. Eng. Sci.* **2008**, *63*, 4171–4175. [CrossRef]
19. Maghsoudi, H. Comparative study of adsorbents performance in ethylene/ethane separation. *Adsorption* **2016**, *22*, 985–992. [CrossRef]
20. Liang, B.; Zhang, X.; Xie, Y.; Lin, R.-B.; Krishna, R.; Cui, H.; Li, Z.; Shi, Y.; Wu, H.; Zhou, W. An ultramicroporous metal–organic framework for high sieving separation of propylene from propane. *J. Am. Chem. Soc.* **2020**, *142*, 17795–17801. [CrossRef]
21. Li, J.; Jiang, L.; Chen, S.; Kirchon, A.; Li, B.; Li, Y.; Zhou, H.-C. Metal–organic framework containing planar metal-binding sites: Efficiently and cost-effectively enhancing the kinetic separation of C₂H₂/C₂H₄. *J. Am. Chem. Soc.* **2019**, *141*, 3807–3811. [CrossRef]
22. Chuah, C.Y.; Li, W.; Yang, Y.; Bae, T.-H. Evaluation of porous adsorbents for CO₂ capture under humid conditions: The importance of recyclability. *Chem. Eng. J. Adv.* **2020**, *3*, 100021. [CrossRef]
23. Chuah, C.Y.; Goh, K.; Yang, Y.; Gong, H.; Li, W.; Karahan, H.E.; Guiver, M.D.; Wang, R.; Bae, T.-H. Harnessing filler materials for enhancing biogas separation membranes. *Chem. Rev.* **2018**, *118*, 8655–8769. [CrossRef]
24. Gong, H.; Chuah, C.Y.; Yang, Y.; Bae, T.-H. High performance composite membranes comprising Zn(pyraz)₂(SiF₆) nanocrystals for CO₂/CH₄ separation. *J. Ind. Eng. Chem.* **2018**, *60*, 279–285. [CrossRef]
25. Karahan, H.E.; Goh, K.; Zhang, C.; Yang, E.; Yildirim, C.; Chuah, C.Y.; Ahunbay, M.G.; Lee, J.; Tantekin-Ersolmaz, Ş.B.; Chen, Y. MXene materials for designing advanced separation membranes. *Adv. Mater.* **2020**, *32*, 1906697. [CrossRef] [PubMed]
26. Robeson, L.M. The upper bound revisited. *J. Membr. Sci.* **2008**, *320*, 390–400. [CrossRef]
27. Robeson, L.M. Correlation of separation factor versus permeability for polymeric membranes. *J. Membr. Sci.* **1991**, *62*, 165–185. [CrossRef]
28. Samarasinghe, S.; Chuah, C.Y.; Yang, Y.; Bae, T.-H. Tailoring CO₂/CH₄ separation properties of mixed-matrix membranes via combined use of two- and three-dimensional metal–organic frameworks. *J. Membr. Sci.* **2018**, *557*, 30–37. [CrossRef]

29. Dou, H.; Jiang, B.; Xu, M.; Zhang, Z.; Wen, G.; Peng, F.; Yu, A.; Bai, Z.; Sun, Y.; Zhang, L. Boron nitride membranes with a distinct nanoconfinement effect for efficient ethylene/ethane separation. *Angew. Chem. Int. Ed.* **2019**, *131*, 14107–14113. [[CrossRef](#)]
30. Rungta, M.; Xu, L.; Koros, W.J. Carbon molecular sieve dense film membranes derived from Matrimid® for ethylene/ethane separation. *Carbon* **2012**, *50*, 1488–1502. [[CrossRef](#)]
31. Li, J.-R.; Kuppler, R.J.; Zhou, H.-C. Selective gas adsorption and separation in metal–organic frameworks. *Chem. Soc. Rev.* **2009**, *38*, 1477–1504. [[CrossRef](#)]
32. Chuah, C.Y.; Lee, H.; Bae, T.-H. Recent advances of nanoporous adsorbents for light hydrocarbon (C₁–C₃) separation. *Chem. Eng. J.* **2022**, *430*, 132654. [[CrossRef](#)]
33. Najari, S.; Saeidi, S.; Gallucci, F.; Drioli, E. Mixed matrix membranes for hydrocarbons separation and recovery: A critical review. *Rev. Chem. Eng.* **2019**, *37*, 363–406. [[CrossRef](#)]
34. Yang, L.; Qian, S.; Wang, X.; Cui, X.; Chen, B.; Xing, H. Energy-efficient separation alternatives: Metal–organic frameworks and membranes for hydrocarbon separation. *Chem. Soc. Rev.* **2020**, *49*, 5359–5406. [[CrossRef](#)] [[PubMed](#)]
35. Chuah, C.Y.; Jiang, X.; Goh, K.; Wang, R. Recent progress in mixed-matrix membranes for hydrogen separation. *Membranes* **2021**, *11*, 666. [[CrossRef](#)] [[PubMed](#)]
36. Burns, R.L.; Koros, W.J. Defining the challenges for C₃H₆/C₃H₈ separation using polymeric membranes. *J. Membr. Sci.* **2003**, *211*, 299–309. [[CrossRef](#)]
37. Rungta, M.; Zhang, C.; Koros, W.J.; Xu, L. Membrane-based ethylene/ethane separation: The upper bound and beyond. *AIChE J.* **2013**, *59*, 3475–3489. [[CrossRef](#)]
38. Naghsh, M.; Sadeghi, M.; Moheb, A.; Chenar, M.P.; Mohagheghian, M. Separation of ethylene/ethane and propylene/propane by cellulose acetate–silica nanocomposite membranes. *J. Membr. Sci.* **2012**, *423*, 97–106. [[CrossRef](#)]
39. Davoodi, S.M.; Sadeghi, M.; Naghsh, M.; Moheb, A. Olefin–paraffin separation performance of polyimide Matrimid®/silica nanocomposite membranes. *RSC Adv.* **2016**, *6*, 23746–23759. [[CrossRef](#)]
40. Ploegmakers, J.; Japip, S.; Nijmeijer, K. Mixed matrix membranes containing MOFs for ethylene/ethane separation Part A: Membrane preparation and characterization. *J. Membr. Sci.* **2013**, *428*, 445–453. [[CrossRef](#)]
41. Chuah, C.Y.; Bae, T.-H. Incorporation of Cu₃BTC₂ nanocrystals to increase the permeability of polymeric membranes in O₂/N₂ separation. *BMC Chem. Eng.* **2019**, *1*, 2. [[CrossRef](#)]
42. Bachman, J.E.; Smith, Z.P.; Li, T.; Xu, T.; Long, J.R. Enhanced ethylene separation and plasticization resistance in polymer membranes incorporating metal–organic framework nanocrystals. *Nat. Mater.* **2016**, *15*, 845–849. [[CrossRef](#)]
43. Bae, T.-H.; Long, J.R. CO₂/N₂ separations with mixed-matrix membranes containing Mg₂(dobdc) nanocrystals. *Energy Environ. Sci.* **2013**, *6*, 3565–3569. [[CrossRef](#)]
44. Chuah, C.Y.; Samarasinghe, S.A.S.C.; Li, W.; Goh, K.; Bae, T.-H. Leveraging nanocrystal HKUST-1 in mixed-matrix membranes for ethylene/ethane separation. *Membranes* **2020**, *10*, 74. [[CrossRef](#)] [[PubMed](#)]
45. Qian, S.; Xia, L.; Yang, L.; Wang, X.; Suo, X.; Cui, X.; Xing, H. Defect-free mixed-matrix membranes consisting of anion-pillared metal-organic frameworks and poly (ionic liquid)s for separation of acetylene from ethylene. *J. Membr. Sci.* **2020**, *611*, 118329. [[CrossRef](#)]
46. Tomé, L.C.; Guerreiro, D.C.; Teodoro, R.M.; Alves, V.D.; Marrucho, I.M. Effect of polymer molecular weight on the physical properties and CO₂/N₂ separation of pyrrolidinium-based poly (ionic liquid) membranes. *J. Membr. Sci.* **2018**, *549*, 267–274. [[CrossRef](#)]
47. Cowan, M.G.; Masuda, M.; McDanel, W.M.; Kohno, Y.; Gin, D.L.; Noble, R.D. Phosphonium-based poly (Ionic liquid) membranes: The effect of cation alkyl chain length on light gas separation properties and Ionic conductivity. *J. Membr. Sci.* **2016**, *498*, 408–413. [[CrossRef](#)]
48. Ye, L.; Wan, L.; Tang, J.; Li, Y.; Huang, F. Novolac-based poly(1,2,3-triazolium) s with good ionic conductivity and enhanced CO₂ permeation. *RSC Adv.* **2018**, *8*, 8552–8557. [[CrossRef](#)]
49. Li, W.; Chuah, C.Y.; Kwon, S.; Goh, K.; Wang, R.; Na, K.; Bae, T.-H. Nanosizing zeolite 5A fillers in mixed-matrix carbon molecular sieve membranes to improve gas separation performance. *Chem. Eng. J. Adv.* **2020**, *2*, 100016. [[CrossRef](#)]
50. Li, W.; Chuah, C.Y.; Bae, T.-H. Hierarchical 5A Zeolite-Containing Carbon Molecular Sieve Membranes for O₂/N₂ Separation. *Membr. J.* **2020**, *30*, 260–268. [[CrossRef](#)]
51. Tirouni, I.; Sadeghi, M.; Pakizeh, M. Separation of C₃H₈ and C₂H₆ from CH₄ in polyurethane–zeolite 4Å and ZSM-5 mixed matrix membranes. *Sep. Purif. Technol.* **2015**, *141*, 394–402. [[CrossRef](#)]
52. Li, W.; Goh, K.; Chuah, C.Y.; Bae, T.-H. Mixed-matrix carbon molecular sieve membranes using hierarchical zeolite: A simple approach towards high CO₂ permeability enhancements. *J. Membr. Sci.* **2019**, *588*, 117220. [[CrossRef](#)]
53. Chuah, C.Y.; Lee, J.; Bao, Y.; Song, J.; Bae, T.-H. High-performance porous carbon-zeolite mixed-matrix membranes for CO₂/N₂ separation. *J. Membr. Sci.* **2021**, *622*, 119031. [[CrossRef](#)]
54. Chuah, C.Y.; Anwar, S.N.B.M.; Weerachanchai, P.; Bae, T.-H.; Goh, K.; Wang, R. Scaling-up defect-free asymmetric hollow fiber membranes to produce oxygen-enriched gas for integration into municipal solid waste gasification process. *J. Membr. Sci.* **2021**, *640*, 119787. [[CrossRef](#)]
55. Chuah, C.Y.; Goh, K.; Bae, T.-H. Enhanced performance of carbon molecular sieve membranes incorporating zeolite nanocrystals for air separation. *Membranes* **2021**, *11*, 489. [[CrossRef](#)]

56. Chen, G.; Chen, X.; Pan, Y.; Ji, Y.; Liu, G.; Jin, W. M-gallate MOF/6FDA-polyimide mixed-matrix membranes for C₂H₄/C₂H₆ separation. *J. Membr. Sci.* **2021**, *620*, 118852. [[CrossRef](#)]
57. Min, B.; Yang, S.; Korde, A.; Jones, C.W.; Nair, S. Single-Step Scalable Fabrication of Zeolite MFI Hollow Fiber Membranes for Hydrocarbon Separations. *Adv. Mater. Int.* **2020**, *7*, 2000926. [[CrossRef](#)]
58. Kunjattu, S.H.; Ashok, V.; Bhaskar, A.; Pandare, K.; Banerjee, R.; Kharul, U.K. ZIF-8@ DBzPBI-BuI composite membranes for olefin/paraffin separation. *J. Membr. Sci.* **2018**, *549*, 38–45. [[CrossRef](#)]
59. Ploegmakers, J.; Japip, S.; Nijmeijer, K. Mixed matrix membranes containing MOFs for ethylene/ethane separation—Part B: Effect of Cu₃BTC₂ on membrane transport properties. *J. Membr. Sci.* **2013**, *428*, 331–340. [[CrossRef](#)]
60. Higuchi, A.; Agatsuma, T.; Uemiya, S.; Kojima, T.; Mizoguchi, K.; Pinnau, I.; Nagai, K.; Freeman, B.D. Preparation and gas permeation of immobilized fullerene membranes. *J. Appl. Polym. Sci.* **2000**, *77*, 529–537. [[CrossRef](#)]
61. Díaz, K.; López-González, M.; del Castillo, L.F.; Riande, E. Effect of zeolitic imidazolate frameworks on the gas transport performance of ZIF8-poly(1,4-phenylene ether-ether-sulfone) hybrid membranes. *J. Membr. Sci.* **2011**, *383*, 206–213. [[CrossRef](#)]
62. Jiang, B.; Zhou, J.; Xu, M.; Dou, H.; Zhang, H.; Yang, N.; Zhang, L. Multifunctional ternary deep eutectic solvent-based membranes for the cost-effective ethylene/ethane separation. *J. Membr. Sci.* **2020**, *610*, 118243. [[CrossRef](#)]
63. Park, K.S.; Ni, Z.; Côté, A.P.; Choi, J.Y.; Huang, R.; Uribe-Romo, F.J.; Chae, H.K.; O’Keeffe, M.; Yaghi, O.M. Exceptional chemical and thermal stability of zeolitic imidazolate frameworks. *Proc. Natl. Acad. Sci. USA* **2006**, *103*, 10186–10191. [[CrossRef](#)]
64. Zhang, C.; Lively, R.P.; Zhang, K.; Johnson, J.R.; Karvan, O.; Koros, W.J. Unexpected molecular sieving properties of zeolitic imidazolate framework-8. *J. Phys. Chem. Lett.* **2012**, *3*, 2130–2134. [[CrossRef](#)] [[PubMed](#)]
65. Vinh-Thang, H.; Kaliaguine, S. Predictive models for mixed-matrix membrane performance: A review. *Chem. Rev.* **2013**, *113*, 4980–5028. [[CrossRef](#)] [[PubMed](#)]
66. Zhang, C.; Dai, Y.; Johnson, J.R.; Karvan, O.; Koros, W.J. High performance ZIF-8/6FDA-DAM mixed matrix membrane for propylene/propane separations. *J. Membr. Sci.* **2012**, *389*, 34–42. [[CrossRef](#)]
67. Chuah, C.Y.; Goh, K.; Bae, T.-H. Hierarchically structured HKUST-1 nanocrystals for enhanced SF₆ capture and recovery. *J. Phys. Chem. C* **2017**, *121*, 6748–6755. [[CrossRef](#)]
68. Zhang, C.; Zhang, K.; Xu, L.; Labreche, Y.; Kraftschik, B.; Koros, W.J. Highly scalable ZIF-based mixed-matrix hollow fiber membranes for advanced hydrocarbon separations. *AIChE J.* **2014**, *60*, 2625–2635. [[CrossRef](#)]
69. Ma, X.; Swaidan, R.J.; Wang, Y.; Hsiung, C.-e.; Han, Y.; Pinnau, I. Highly compatible hydroxyl-functionalized microporous polyimide-ZIF-8 mixed matrix membranes for energy efficient propylene/propane separation. *ACS Appl. Nano Mater.* **2018**, *1*, 3541–3547. [[CrossRef](#)]
70. Fang, M.; Wu, C.; Yang, Z.; Wang, T.; Xia, Y.; Li, J. ZIF-8/PDMS mixed matrix membranes for propane/nitrogen mixture separation: Experimental result and permeation model validation. *J. Membr. Sci.* **2015**, *474*, 103–113. [[CrossRef](#)]
71. Liu, D.; Xiang, L.; Chang, H.; Chen, K.; Wang, C.; Pan, Y.; Li, Y.; Jiang, Z. Rational matching between MOFs and polymers in mixed matrix membranes for propylene/propane separation. *Chem. Eng. Sci.* **2019**, *204*, 151–160. [[CrossRef](#)]
72. Kwon, H.T.; Jeong, H.-K.; Lee, A.S.; An, H.S.; Lee, J.S. Heteroepitaxially grown zeolitic imidazolate framework membranes with unprecedented propylene/propane separation performances. *J. Am. Chem. Soc.* **2015**, *137*, 12304–12311. [[CrossRef](#)]
73. Pimentel, B.R.; Parulkar, A.; Zhou, E.k.; Brunelli, N.A.; Lively, R.P. Zeolitic imidazolate frameworks: Next-generation materials for energy-efficient gas separations. *ChemSusChem* **2014**, *7*, 3202–3240. [[CrossRef](#)]
74. Krokidas, P.; Castier, M.; Moncho, S.; Sredojevic, D.N.; Brothers, E.N.; Kwon, H.T.; Jeong, H.-K.; Lee, J.S.; Economou, I.G. ZIF-67 framework: A promising new candidate for propylene/propane separation. experimental data and molecular simulations. *J. Phys. Chem. C* **2016**, *120*, 8116–8124. [[CrossRef](#)]
75. An, H.; Park, S.; Kwon, H.T.; Jeong, H.-K.; Lee, J.S. A new superior competitor for exceptional propylene/propane separations: ZIF-67 containing mixed matrix membranes. *J. Membr. Sci.* **2017**, *526*, 367–376. [[CrossRef](#)]
76. Oh, J.W.; Cho, K.Y.; Kan, M.-Y.; Yu, H.J.; Kang, D.-Y.; Lee, J.S. High-flux mixed matrix membranes containing bimetallic zeolitic imidazole framework-8 for C₃H₆/C₃H₈ separation. *J. Membr. Sci.* **2020**, *596*, 117735. [[CrossRef](#)]
77. Moghadam, F.; Lee, T.H.; Park, I.; Park, H.B. Thermally annealed polyimide-based mixed matrix membrane containing ZIF-67 decorated porous graphene oxide nanosheets with enhanced propylene/propane selectivity. *J. Membr. Sci.* **2020**, *603*, 118019. [[CrossRef](#)]
78. Chuah, C.Y.; Lee, J.; Bae, T.-H. Graphene-based Membranes for H₂ Separation: Recent Progress and Future Perspective. *Membranes* **2020**, *10*, 336. [[CrossRef](#)]
79. Li, W.; Chuah, C.Y.; Yang, Y.; Bae, T.-H. Nanocomposites formed by in situ growth of NiDOBDC nanoparticles on graphene oxide sheets for enhanced CO₂ and H₂ storage. *Micropor. Mesopor. Mater.* **2018**, *265*, 35–42. [[CrossRef](#)]
80. Li, W.; Chuah, C.Y.; Nie, L.; Bae, T.-H. Enhanced CO₂/CH₄ selectivity and mechanical strength of mixed-matrix membrane incorporated with NiDOBDC/GO composite. *J. Ind. Eng. Chem.* **2019**, *74*, 118–125. [[CrossRef](#)]
81. Liu, Y.; Chen, Z.; Liu, G.; Belmabkhout, Y.; Adil, K.; Eddaoudi, M.; Koros, W. Conformation-controlled molecular sieving effects for membrane-based propylene/propane separation. *Adv. Mater.* **2019**, *31*, 1807513. [[CrossRef](#)]
82. Lee, T.H.; Jung, J.G.; Kim, Y.J.; Roh, J.S.; Yoon, H.W.; Ghanem, B.S.; Kim, H.W.; Cho, Y.H.; Pinnau, I.; Park, H.B. Defect Engineering in Metal–Organic Frameworks Towards Advanced Mixed Matrix Membranes for Efficient Propylene/Propane Separation. *Angew. Chem. Int. Ed.* **2021**, *133*, 13191–13198. [[CrossRef](#)]

83. Chuah, C.Y.; Lee, J.; Song, J.; Bae, T.-H. CO₂/N₂ separation properties of polyimide-based mixed-matrix membranes comprising UiO-66 with various functionalities. *Membranes* **2020**, *10*, 154. [[CrossRef](#)]
84. Park, C.H.; Lee, J.H.; Jung, J.P.; Kim, J.H. Mixed matrix membranes based on dual-functional MgO nanosheets for olefin/paraffin separation. *J. Membr. Sci.* **2017**, *533*, 48–56. [[CrossRef](#)]
85. Sun, H.; Ma, C.; Wang, T.; Xu, Y.; Yuan, B.; Li, P.; Kong, Y. Preparation and characterization of C₆₀-filled ethyl cellulose mixed-matrix membranes for gas separation of propylene/propane. *Chem. Eng. Technol.* **2014**, *37*, 611–619. [[CrossRef](#)]
86. Heidari, M.; Hosseini, S.S.; Nasrin, M.O.; Ghadimi, A. Synthesis and fabrication of adsorptive carbon nanoparticles (ACNs)/PDMS mixed matrix membranes for efficient CO₂/CH₄ and C₃H₈/CH₄ separation. *Sep. Purif. Technol.* **2019**, *209*, 503–515. [[CrossRef](#)]
87. Beltran, A.B.; Nisola, G.M.; Cho, E.; Lee, E.E.D.; Chung, W.-J. Organosilane modified silica/polydimethylsiloxane mixed matrix membranes for enhanced propylene/nitrogen separation. *Appl. Surf. Sci.* **2011**, *258*, 337–345. [[CrossRef](#)]
88. Yang, F.; Mu, H.; Wang, C.; Xiang, L.; Yao, K.X.; Liu, L.; Yang, Y.; Han, Y.; Li, Y.; Pan, Y. Morphological map of ZIF-8 crystals with five distinctive shapes: Feature of filler in mixed-matrix membranes on C₃H₆/C₃H₈ separation. *Chem. Mater.* **2018**, *30*, 3467–3473. [[CrossRef](#)]
89. Jeong, S.; Kang, S.W. Effect of Ag₂O nanoparticles on long-term stable polymer/AgBF₄/Al(NO₃)₃ complex membranes for olefin/paraffin separation. *Chem. Eng. J.* **2017**, *327*, 500–504. [[CrossRef](#)]
90. Yoon, K.W.; Kang, Y.S.; Kang, S.W. Activated Ag ions and enhanced gas transport by incorporation of KIT-6 for facilitated olefin transport membranes. *J. Membr. Sci.* **2016**, *513*, 95–100. [[CrossRef](#)]
91. Chuah, C.Y.; Li, W.; Samarasinghe, S.; Sethunga, G.; Bae, T.-H. Enhancing the CO₂ separation performance of polymer membranes via the incorporation of amine-functionalized HKUST-1 nanocrystals. *Micropor. Mesopor. Mater.* **2019**, *290*, 109680. [[CrossRef](#)]
92. Li, P.; Chung, T.-S.; Paul, D. Gas sorption and permeation in PIM-1. *J. Membr. Sci.* **2013**, *432*, 50–57. [[CrossRef](#)]
93. Luque-Alled, J.M.; Ameen, A.W.; Alberto, M.; Tamaddondar, M.; Foster, A.B.; Budd, P.M.; Vijayaraghavan, A.; Gorgojo, P. Gas separation performance of MMMs containing (PIM-1)-functionalized GO derivatives. *J. Membr. Sci.* **2021**, *623*, 118902. [[CrossRef](#)]